Biotechnology Reports 6 (2015) 27–35

Contents lists available at ScienceDirect

Biotechnology Reports

journal homepage: www.elsevier.com/locate/btre

Improving the biophysical properties of anti-ricin single-domain antibodies☆

Kendrick B. Turner [a], Jinny L. Liu [b], Dan Zabetakis [b], Audrey Brozozog Lee [c], George P. Anderson [b], Ellen R. Goldman [b,*]

[a] American Society for Engineering Education, Postdoctoral Fellow at the Naval Research Laboratory, Washington, DC 20375, USA
[b] Center for Biomolecular Science and Engineering, Naval Research Laboratory, Washington, DC 20375, USA
[c] NOVA Research Inc., 1900 Elkin St. Suite 230, Alexandria, VA 22308, USA

ARTICLE INFO

Article history:
Received 23 December 2014
Accepted 13 January 2015
Available online 15 January 2015

Keywords:
Thermostability
Circular dichroism
Camelid

ABSTRACT

Single-domain antibodies (sdAbs) derived from heavy-chain only antibodies produced in camelids are attractive immunoreagents due to their small size, high affinity, and ability to refold and retain binding activity after denaturation. It has been observed that some sdAbs, however, exhibit undesirable properties including reduced solubility when subjected to heating or upon long-term storage at production-relevant concentrations, which can limit their usefulness. Using a multi-step, rational design approach that included consensus-sequence driven sequence repairs, the alteration of net protein charge, and the introduction of non-native disulfide bonds, augmented solubility and increased melting temperatures were achieved. The improved sdAbs tolerated storage in solution at high concentration (10 mg/mL) and were able to withstand multiple cycles of heating to high temperature (70 °C). This work demonstrates a pathway for improving the biophysical characteristics of sdAbs which is essential for expanding their utility for both diagnostic as well as therapeutic applications.

1. Introduction

There is an ongoing need for the development of robust recognition reagents for the sensitive detection of potential biothreat agents as well as new and emerging pathogens. Traditionally, biosensors utilizing antibody recognition elements have provided reliable detection capability for a broad range of targets; however, antibodies are prone to failure when exposed to harsh environments. Recombinantly-expressed binding domains derived from the remarkable heavy-chain-only antibodies produced by camelids (such as camels and llamas), termed single-domain antibodies (sdAbs), offer alternative binding elements. sdAbs provide the affinity and specificity of traditional antibodies, as well as additional desirable properties [1–4]. Importantly, many sdAbs have been demonstrated to refold into an active form able to bind antigen after heating to high temperatures [5–7]. Additionally, their small size (1/10 that of conventional antibodies), ability to bind "hidden" epitopes by virtue of an extended CDR3 region, and ability to be rationally-selected and produced in quantity by standard recombinant protein expression manufacturing methods make sdAbs attractive immunoreagents [1–4].

Unlike traditional antibodies, which normally aggregate and lose their ability to function after being heated above their melting temperature (T_m; the temperature at which half the protein is unfolded) [8], sdAbs are often found to recover their binding ability even after repeated thermal denaturation [5,7]. However, when heated above their melting temperature at high concentration and for extended periods of time, many sdAb clones are prone to aggregation [9]. As aggregation is also a problem with scFvs, recombinant binding domains derived from conventional antibodies, several strategies have been reported that led to more soluble and stable recombinant antibody-binding domains (rAbs). One successful strategy has been to produce sdAbs as fusions with a thermostable protein, as demonstrated by a fusion between a sdAb and a thermostable maltose binding protein that was able to withstand heating to 70 °C for an hour without loss of activity [10]. Increasing the net charge of the protein also can lead to more soluble rAbs. This can be accomplished by either appending a charged tail onto the rAb [9] or the substitution of charged amino acids in the protein sequence [11–16].

Researchers have also investigated schemes to increase the T_m of rAbs. For example, the T_m of a sdAb was increased through the process of random mutagenesis coupled with a stringent selection, which led to a ~7 °C increase in T_m to 90 °C [17]. Grafting the

* Corresponding author. Tel.: +1 202 404 6052.
E-mail address: ellen.goldman@nrl.navy.mil (E.R. Goldman).

http://dx.doi.org/10.1016/j.btre.2015.01.001

antigen binding loops (complementarity determining regions; CDRs) onto a more stable rAb framework has also provided increases in T_m and stability [18–21]. Finally, the introduction of a pair of cysteine residues in frameworks 2 and 3 of sdAbs is another method that has yielded sdAb variants with higher T_ms [22–25].

Although most sdAbs are already more soluble and thermally stable than conventional antibodies or their recombinantly expressed binding domains (i.e., scFv), enhancing the ability of sdAbs to retain binding activity after a heat challenge is a useful metric towards the goal of improving the performance of field portable detection devices in austere environments. To accomplish this metric, we started with previously described high-affinity sdAbs specific for three distinct epitopes on ricin [26,27], and implemented a multi-step process for obtaining binders with improved melting temperature and solubility. Ricin is a potent toxin listed as a select agent by the CDC, and the ability to detect ricin remains a high priority [28–31]. The potential offered by these thermal stabilized sdAb reagents to eliminate the cold-chain makes them a highly attractive alternative to conventional monoclonal antibody and scFv binding reagents. These sdAbs have the potential to provide more consistent function, while their ease of production could make their production less costly than conventional antibodies. Demonstrating excellent thermostability is the first step towards eliminating the need for refrigeration of these reagents – a big plus for forward-based troops or first-responders who could then keep their detection reagents at ambient temperature without negatively impacting shelf-life.

2. Materials and methods

2.1. Reagents

Ricin was purchased from Vector Laboratories. The reagents 1-ethyl-3-(3-dimethylaminopropyl)-carbodiimide hydrochloride (EDC), *N*-hydroxysulfosuccinimide (sulfo-NHS), and NHS-LC-LC-biotin were purchased from Pierce. Anti-ricin sdAbs were described previously [26,27]. Enzymes used for cloning were from New England Biolabs. DNA sequencing services were provided by Eurofins Genomics. Oligos were also purchased from Eurofins Genomics. Mutagenesis was carried out using the QuickChange Site Directed Mutagenesis Kit or QuikChange Multi Site-Directed Mutagenesis Kit from Agilent Technologies. Sequence alignments were performed using MultAlin [32]. Unless otherwise specified, chemical reagents were from Sigma Aldrich, Fisher Scientific, or VWR International.

2.2. Selection

Additional ricin clones were selected from our previously described immune library using essentially the same protocol previously employed [26]. Two rounds of panning were performed, and then binding phage were identified by monoclonal phage ELISA as described previously [26].

2.3. Introduction of negatively charged amino acids

Negatively charged amino acids were introduced into the sequences for C10, D12f, and H1W by multisite-directed mutagenesis using the following primers (5′–3′): GGAGGATTGGTGCAGGATGGGGGCTCTCTGAGA, AGGATATCGTATGCGGATTCCGTGAAGGGCCGA, and AGCGACAACTGGAAGAACACGGTGTATCTGCAA (C10); GTCACAGACTATGCAGATTCCGTGAAGGGTCGA and GCTAGTAGAAACTCGGATGACTATGGTTACTGG (D12f); and GGAGGATTGGCGCAGGATGGGGGTTCTCTCCGA and CAGGCTCCAGGGAAGGAACGTGAGTTTGTGGCT (H1W). Mutagenesis reactions were carried out as described in the product protocol and mutants were identified and confirmed by DNA sequencing.

2.4. Introduction of additional disulfide bond

The introduction of an additional disulfide bond in each of the sdAbs was accomplished by site-directed mutagenesis using the following primers and their reverse complements: GAGCGTGAATTTGTCTGCGTTATTAGTGGTTCT and AAGGGTCGATTCACCTGCTCCAGAGACGTCGCC (D12neg), GAACGTGAGTTTGTGTGCGCAATTAGGGCGAGA and AAGGGGCGATTCACCTGCTCCAGAGACAACGGC (H1Wneg), and GAGCGTGAGTTTGTTTGCGCACTTCGGTGGACT and AAGGGCCGATTCACCTGCTCCAGCGACAACTGG (C10neg). Following mutagenesis, the presence of an additional pair of cysteines was confirmed by sequencing.

2.5. Protein production

A PCR strategy was utilized to remove the upper hinge sequence; the sdAbs were cloned into pet22b for expression in the periplasm [33]. Bacteria were grown and protein purified as described [9,17]. Briefly, protein was purified through immobilized metal affinity chromatography and size exclusion. Protein concentration was determined by absorbance at 280 nm on a NanoDrop spectrophotometer.

2.6. Fluorescence based melting assay

The fluorescence based melting assay was conducted using an Applied Biosystems StepOne Real-Time PCR system and Sypro Orange dye (Sigma) [33]. A total of 10 μg of each purified sdAb was added to a 20 μL volume of PBS buffer. The Sypro Orange dye was diluted 1000-fold into each reaction solution. The temperature was increased from 25 to 99 °C at a rate of 1.2 °C/min. All measurements were done in triplicate and the values agreed within 0.6 °C.

2.7. T_m determination by circular dichroism

Refolding and melting temperatures were assessed using a Jasco J-815 circular dichroism (CD) spectrometer [33,34]. Samples were diluted with deionized water to a final concentration of 40 μg/mL. The differential absorbance of the protein sample was measured at 205 nm to monitor the secondary structure of the protein as the temperature was increased from 25 to 90 °C incrementally at a rate of 2.5 °C/min. The melting point correlated to the temperature at the inflection point between the folded and unfolded state. Ellipticity was recorded as samples were cooled to determine the refolding ability. The error on the T_m determinations was within ±1 °C.

2.8. Evaluation of aggregation

To evaluate the degree of aggregation, sdAbs were prepared at a concentration of 1.0 mg/mL (as measured by OD_{280} using a NanoDrop spectrophotometer) in PBS and incubated for 1 h at a range of temperatures (25, 57, 72, and 87 °C). A second experiment to determine the degree of aggregation resulting from thermal cycling was performed by preparing sdAbs at a concentration of 1.0 mg/mL and then subjecting them to 10 cycles of heating to 70 °C for 30 min followed by cooling to 25 °C for 30 min. Following incubation or thermal cycling, samples were centrifuged to pellet any precipitated protein and the concentration was measured again on the NanoDrop to quantify remaining soluble protein.

2.9. Surface plasmon resonance (SPR)

A BioRad ProteOn XPR36 system and standard GLC sensor chip was used to assess binding kinetics. Ricin was immobilized to the sensor chip surface on four rows at a saturating concentration of

10 μg/mL using EDC/NHS chemistry. Protein was flowed over the activated surface for 300 s at a flow rate of 30 μL/min. The surface was inactivated with ethanolamine. To determine binding kinetics, the chip was turned 90°, then 3-fold dilutions (300–0 nM) of each sdAb were flowed across the chip for 90 or 120 s at 100 μL/min and binding was recorded on the ricin-coated lanes; next, the buffer was flowed over for 600 s and the dissociation monitored. The surface was regenerated with either 50 mM glycine (pH 2.5) or 1% phosphoric acid between individual samples. The one shot kinetics was determined from each of the ricin-coated rows using five concentrations of single-domain antibody. Kinetic parameters were calculated using the ProteOn Manager RM 2.1 software. The average values determined are shown in Table 1. The range of values from the four measurements was always within a factor of 2, and typically the four values were within 20%.

2.10. MAGPIX

Sandwich assays were used to characterize the utility of the thermal stabilized sdAbs for the detection of ricin, and were performed similar to assays described previously [34,35], however with an amplification step [36]. The sdAbs (≥1 mg/mL) were immobilized to MagPlex beads covalently using EDC/NHS reagents and the standard two step protocol provided by the manufacturer. The sdAbs were also biotinylated (Bt) using a 5× concentration sulfo NHS-LC-LC-biotin (Pierce) reagent. Free biotin was removed using Zeba spin 7K desalting columns (Thermo).

The anti-ricin sdAb-coated microspheres were added to ricin dilutions prepared in PBST with 1% BSA (PBSTB) in vertical columns of a 96 well polypropylene round bottom microtiter plate. PBSTB was used for all reagent dilutions and PBST for the wash steps. After a 30 min incubation at room temperature in the dark, unbound ricin was removed by placing the plate on a 96f magnet (BioTek) and washing three times. The microsphere were then resuspended in PBSTB and distributed into a different vertical column for each Bt-sdAb detection antibody to be tested. The Bt-sdAb (2 μg/mL final) was added to each well of its column. After a 30 min incubation the plate was washed three times to remove unbound Bt-sdAb. To complete the amplified fluorescent sandwich assay, a streptavidin conjugated phycoerythrin (SAPE, Columbia Biosciences) was used as the reporter at a concentration of 2.5 μg/mL for 15 min, followed by Bt-goat anti-streptavidin (1 μg/mL, Vector Labs) for 15 min, and a final incubation with SAPE as before, with three washes in between and afterwards. The microspheres were resuspended in 75 μL of PBST and evaluated on the MAGPIX instrument (Luminex). Binding was measured from greater than 50 beads; the error of the mean fluorescence intensity (MFI) was found to be 5% or less. The sandwich assays were performed on at least two different days, and in each case, the experimental data replicated.

3. Results and discussion

3.1. Identifying starting sequences

3.1.1. Evaluation of T_ms of high affinity sdAbs isolated in original library panning

When we originally isolated ricin binders from a phage-display library derived from two llamas that had been immunized with ricin toxoid, we found several sequence families, each containing multiple members [26]. Members of each sequence family shared sequence homology through their CDR regions (Fig. 1A) and competed with each other for binding to toxin, indicating a common epitope among family members. We prepared many of the identified proteins for evaluation of their binding kinetics then chose representatives of three families that showed excellent affinity and that bound to distinct epitopes on ricin (epitopes 1, 2, and 3) to more fully characterize and to integrate into assays for ricin detection [27]. Although family members may share very similar sequences, it has been observed with sdAbs specific to other targets such as *Bacillus anthracis* and the bacteriophage MS2 that small changes in sequence can result in major differences in T_ms [34,37]. We therefore started our mission to engineer anti-ricin sdAbs that possess high T_ms and resist aggregation by re-visiting the previously identified binders. We used an easily multiplexed dye-based fluorescent melt assay to provide a first estimate of melting temperature followed by CD which provided our standard T_m value (Table 1).

Table 1
T_m and binding kinetics and affinity characteristics of sdAb clones.

Clone	T_m(°C), dye melt	T_m(°C), CD	k_a (1/Ms)	k_d (1/s)	K_D(M)
C2	65	nd	1.5×10^{-9}	2.9×10^{-4}	1.9×10^{-9}
C8	58	60	1.0×10^{6}	2.8×10^{-4}	2.7×10^{-10}
D12	74	76	1.9×10^{5}	1.7×10^{-4}	9.0×10^{-10}
E9	55	58	3.6×10^{5}	6.1×10^{-5}	1.7×10^{-10}
H3	53	57	4.3×10^{5}	9.7×10^{-5}	2.2×10^{-10}
H1	65	65	6.4×10^{4}	3.9×10^{-5}	6.1×10^{-10}
F8	58	59	3.6×10^{5}	4.9×10^{-5}	1.4×10^{-10}
D1	50	49	4.1×10^{5}	3.3×10^{-4}	8.0×10^{-10}
F11	50	54	1.3×10^{5}	1.2×10^{-4}	9.0×10^{10}
D12f	74	78	1.4×10^{6}	6.7×10^{-5}	5.1×10^{-11}
H1W	70	71	2.7×10^{5}	1.5×10^{-4}	5.8×10^{-10}
C10	60	66	1.3×10^{5}	6.1×10^{-4}	4.9×10^{-9}
D12fneg	77	79	1.7×10^{6}	6.9×10^{-5}	4.1×10^{-11}
H1Wneg	62	65	4.6×10^{5}	2.8×10^{-4}	6.2×10^{-10}
C10neg	65	65	2.1×10^{6}	1.3×10^{-4}	6.0×10^{-11}
D12fneg+	77	82	4.8×10^{5}	7.3×10^{-5}	1.5×10^{-10}
H1W+	75	78	4.8×10^{5}	2.1×10^{-3}	4.3×10^{-9}
H1Wneg+	68	75	1.6×10^{6}	5.1×10^{-3}	3.2×10^{-9}
C10neg+	78	78	8.0×10^{5}	3.4×10^{-4}	4.2×10^{-10}

nd: not done.

Fig. 1. Deduced amino acid sequence of mutants. (A) Sequences from original panning. Three sequence families bind to three epitopes. E9 through D12 bind to epitope 1; H1 and F8 bind to epitope 2; D1 and F11 bind to epitope 3. The 4 framework (FW) and 3 CDR regions have been labeled and are indicated by green (FW) and blue (CDR) bars above the sequences. (B) Sequences of D12f, H1W, and C10. The sites of the mutations in D12f and H1W are highlighted by the purple and maroon arrows, respectively. CDRs are indicated by a blue line. (C) Sequence of negative mutants. Red residues were mutated to the amino acid shown in parenthesis. CDRs are indicated by the blue line below the sequence. The pI of the original mutant and the "neg" variant are above each sequence. Positions show in orange, and underlined were mutated to C in constructs designed to have an additional disulfide.

Not surprisingly, a wide range of T_ms was observed within the families. We identified D12 (T_m 76 °C) and H1 (T_m 65 °C), which bind to epitopes 1 and 2, respectively, as potential starting sequences for designing sdAbs with improved characteristics. Both members of the third family recognizing epitope 3 (sdAb F11 and D1), however, possessed very low T_ms of 54 and 49 °C, respectively.

3.1.2. Additional selections to identify clones with higher T_m*s*

Going back to the immune library and performing additional selections offered another route for identifying sequences of ricin-binding sdAbs to serve as starting points for antibody engineering. This panning did not lead to identification of new sequence families, but new members of the existing families were selected and their T_m determined. One of the new clones (C10) is in the same family as the low T_m binders F11 and D1 that binds to epitope 3 (Fig. 1B). Clone C10, however, was found to have a T_m over 10 °C degrees higher than the other two members of this family. Therefore clone C10 was identified as a potential starting sequence of a sdAb recognizing epitope 3.

3.2. Engineering to optimize based on consensus sequence analysis

The D12 sdAb, which binds to epitope 1 on ricin, possessed the highest T_m of its family; however, analysis of its sequence revealed an unpaired Cys in CDR 2. This was reflected in the observation of a sizable dimer peak on purification by size-exclusion chromatography (Supplemental Fig. 1). Other family members have a Ser at that sequence position; therefore site-directed mutagenesis was utilized to make the Cys to Ser change. The resultant "fixed" clone, termed D12f, was found to have the same high affinity as the parental sequence, and the T_m was 2 °C higher, 78 °C as determined by CD. Even more importantly, the yield improved as only the desired monomer product was now produced.

Analyzing the sequence of H1, a sdAb that binds to epitope 2, revealed that in framework 4, an Arg had replace the Trp that is nearly universally conserved among the heavy chains found in rAbs [38]. Restoring the consensus sequence Trp creating clone H1W, resulted in a ~5 °C increase in T_m to 71 °C, without decreasing affinity for ricin or altering the yield.

Epitope 3 binder D1 had a low T_m and an apparent deletion at the end of CDR2 compared to the consensus sequence [38]. Prior to isolating C10, a version of D1 was synthesized that restored the three missing amino acids (Val-Lys-Gly) typically present at the end of CDR 2. The insertion by itself did not raise the ~50 °C T_m of D1. Interestingly sdAb C10, isolated through a new panning, restored the deletion, among other changes, and melted at 66 °C.

3.3. Negative mutations to improve solubility and aggregation resistance

Calculation of the isoelectric point (pI) of the three candidate sequences, D12f, H1W, and C10 produced values of 8.08, 6.64, and 8.65, respectively. We observed that when D12f and C10 were produced and purified at concentrations in excess of 5 mg/L they aggregated and precipitated upon storage in PBS at 4 °C. While these aggregates were reversible upon decreasing the pH of the solution, this poor solubility at neutral pH was clearly an undesirable property for either large scale production or during application. H1W, which has a more negative pI, had no apparent solubility issues. In addition, when examined by CD, D12f, H1W, and C10 all show an ability to refold after melting; however, none of these sdAbs refolded 100% (top panels Fig. 2). This suggested that even at the dilute concentrations used in CD measurements, when heated to 95 °C, a percentage of the sdAb preparation was unable to regain its secondary structure, perhaps due to aggregation. Solutions of the D12f, H1W and C10 sdAbs at a concentration of ~1 mg/mL were subjected to heating to elevated temperatures, even in excess of their T_m. After heating, the sdAbs were centrifuged and protein concentration estimated by the absorbance at 280 nm. As shown in Fig. 3A, the H1W concentration

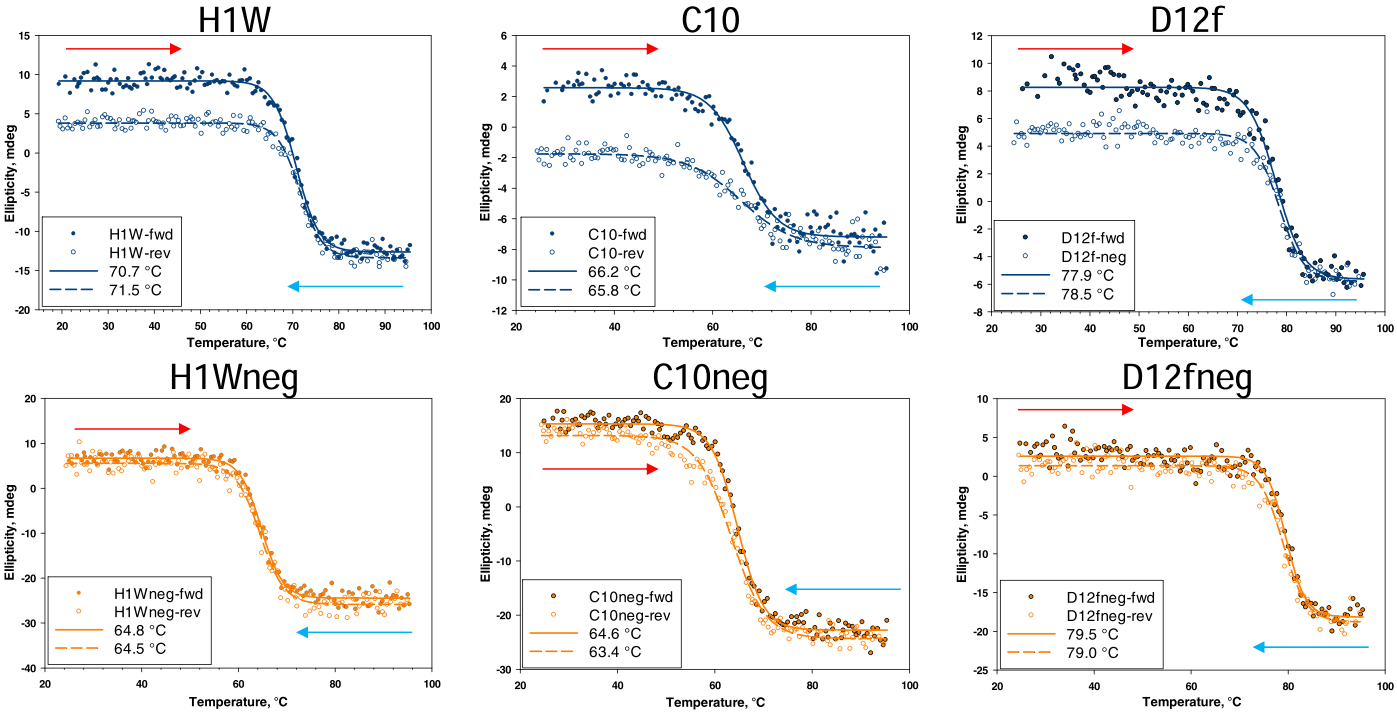

Fig. 2. CD showing T_m and ability of sdAbs to refold. The top panel shows H1W, C10, and D12f which all show some refolding ability, but none regain 100% of its secondary structure. The bottom panels show the negative mutants which all show almost perfect refolding after being heated to 95 °C.

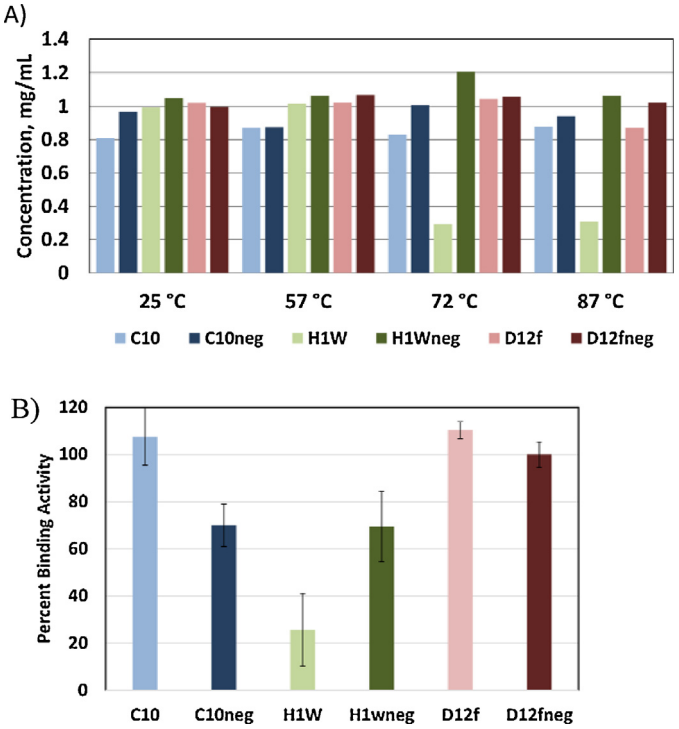

Fig. 3. Aggregation resistance and activity of sdAbs upon incubation at elevated temperatures. (A) The sdAbs were prepared at a concentration of ~ 1 mg/mL, and incubated for 1 h at the indicated temperatures. Following incubation, samples were centrifuged to pellet any precipitated protein, and the final absorbance was measured, as above. (B) The percentage of binding activity remaining after incubation at 72 °C (for C10, C10neg, H1W, and H1Wneg) or 87 °C (for D12f and D12fneg) as described in (A) was determined. Activity was measured in a direct-binding format to ricin immobilized on MagPlex microspheres. Dilutions of each sdAb were added to the MagPlex beads followed by addition of an anti-His tag IgG – R-phycoerythrin (1 μg/mL) for signal generation. Inhibition was evaluated at concentrations on the linear portion of the response curve.

dropped substantially when heated above its T_m, indicating that much of the sdAb had aggregated. It is important to consider that unfolded/misfolded material and smaller aggregates may stay in solution, so the lack of precipitation seen in the other samples does not necessarily correlate with the functionality of the protein remaining in solution, thus remaining binding activity was also evaluated following the solubility determination.

To address the issues of poor solubility and thermal induced aggregation, each protein was subjected to mutagenesis to lower the pI of the sdAb creating the clones D12fneg, H1Wneg, and C10neg (Fig. 1C) which reduced the calculated pI values to 6.72, 6.03, and 6.71, respectively. Positions for the negative mutations were chosen by examining consensus sequences as well as looking at the sequences of other sdAbs in the sequence families. CD revealed that all three negative mutants showed close to 100% ability to refold (bottom panels Fig. 2); the T_m of H1Wneg decreased to 65 °C, while D12fneg and C10neg were essentially unchanged. The sdAbs D12f, H1W, C10, and their negatively charged mutants were prepared at a concentration of ~1 mg/mL and incubated for 1 h at various temperatures followed by determination of the concentration soluble protein remaining in solution (Fig. 3A). The negative mutations dramatically decreased the aggregation shown by H1W, with smaller improvements for C10 and D12f.

Although the negatively charged proteins proved to be more soluble and less prone to aggregation than the parental sdAbs it is critical to ensure that they maintain functionality and are still able to bind antigen after heating. Previously, we had observed conventional antibodies that were still in solution after heating but had lost all antigen binding ability [39]. Binding activity was determined for sdAbs incubated for an hour at a concentration of ~1 mg/mL at temperatures above their T_m (72 °C for C10, C10neg, H1W, and H1Wneg; 87 °C for D12f and D12fneg). Functionality was assayed by direct binding to ricin-coated magnetic microspheres in a MagPlex-based assay (Fig. 3B). While C10neg was shown to lose ~30% more of its binding activity upon heating when compared to C10, H1Wneg was shown to maintain more

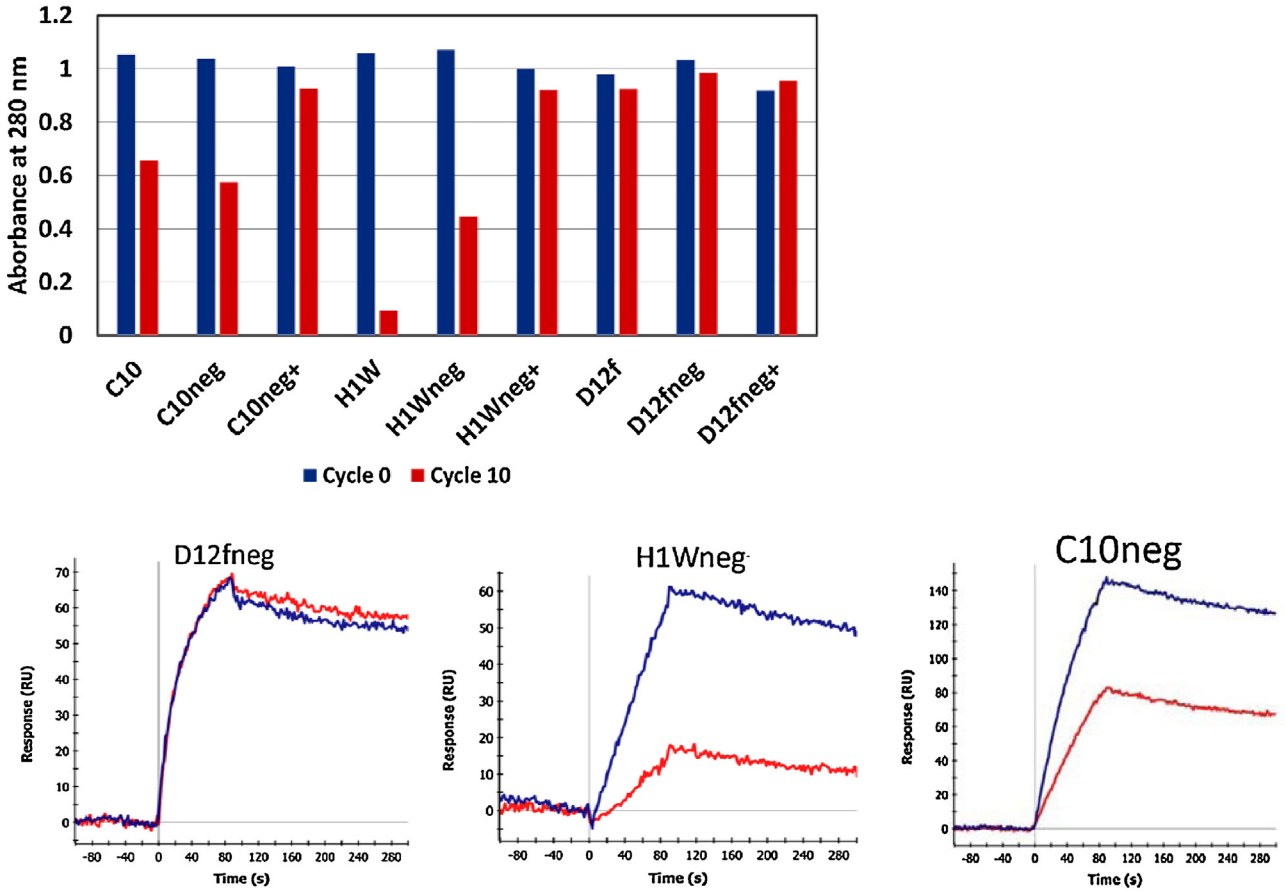

Fig. 4. Aggregation resistance and activity of sdAbs after repeated heating/cooling cycles. (A) The sdAbs were prepared at ~1 mg/mL, and cycled to 70 °C for 30 min followed by 25 °C for 30 min. Following cycling, samples were centrifuged to pellet any precipitated protein, and the final absorbance was measured. (B) The binding ability of the negative mutants after cycling was assessed by SPR, measuring binding of 300 nM sdAb to ricin immobilized on a GLC sensor chip. The blue curve shows binding before cycling, while the red measures binding after.

binding activity (~70%) compared to that of H1W (~25%). D12f and D12fneg both maintained ~100% binding activity even after heating above their T_m.

In a different heat challenge, the proteins, D12fneg, H1Wneg, and C10neg, at a concentration of ~1 mg/mL, were subjected to ten heat cycles during which they were taken up to 70 °C for a half-hour, then cooled to 25 °C for a half-hour. Afterwards, the samples were centrifuged to pellet any precipitated protein, and the absorbance of samples that had been heat cycled was compared to the unheated material (Fig. 4A). Additionally, binding ability was assayed by SPR and showed that whereas D12fneg had maintained ~100% of its activity, C10neg and H1Wneg retained only ~33 and ~20% of their initial binding ability, respectively (Fig. 4B). It is necessary to note that 70 °C is below the T_m of D12fneg but above the T_m of C10neg and H1Wneg. This suggested that even for sdAbs that can refold to retain activity at high concentration and high temperature, maintenance of a folded state is most advantageous.

These results suggested that addition of negative mutations did little to enhance thermal stability, however these mutations were highly effective at enhancing solubility at room temperature, improving sdAb refolding upon denaturation, and facilitating storage at high concentrations. Both the D12f and the C10 precipitated well before they could be concentrated to 10 mg/mL, (~5 mg/mL). However, all three negative mutants were able to be concentrated to ≥10 mg/mL and stayed 100% in solution at room temperature during the 11 day period during which the solutions were monitored (not shown).

3.4. Engineering extra cysteins to improve T_m

In an effort to raise the T_m of sdAbs that recognize each of the 3 epitopes on ricin to over 70 °C, we introduced a pair of Cys placed for formation of an extra disulfide between framework 2 and 3, in the D12fneg, H1W, H1Wneg and C10neg clones (Fig. 1C). This location was chosen as it had previously been demonstrated to increase the stability and T_m of sdAbs [22–24,39,40]. Mutagenesis resulted in the three clones: D12fneg+, H1Wneg+, and C10neg+. The highest increase in T_m was realized with C10neg+ with a T_m of

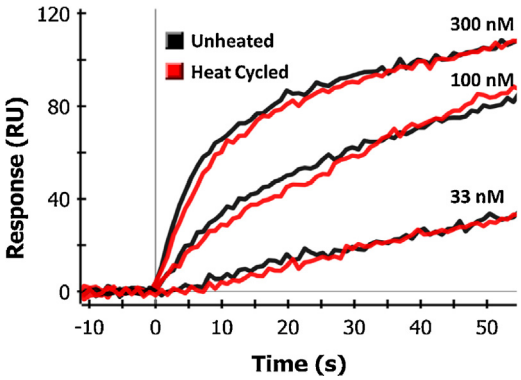

Fig. 5. Function of C10neg+ assessed by SPR before (black) and after (red) heat cycling. The initial binding to ricin is shown for three concentrations of the sdAb.

~78 °C. The H1Wneg+ melting point was increased to 68 °C; adding the disulfide to the original H1W clone to produce H1W+ resulted in a T_m of ~75 °C. The smallest increase was found with D12fneg+, which offered only a minimal increase in T_m. As with the negative mutants, the versions with the added pair of Cys were able to regain ~100% of their secondary structure after heating, as determined by CD (not shown).

The D12fneg+ and C10neg+ were able to recognize ricin with similar high affinity as the parental sdAbs. They were subject to thermal cycling as before, and both maintained near 100% of their binding ability even after 10 cycles up to 70 °C (C10neg+ is shown in Fig. 5). Unfortunately, the increase in T_m that is found with the introduction of an additional disulfide can come at the expense of affinity [23]. The H1Wneg+ and H1W+ clones suffered significant loss of affinity for ricin (Table 1).

3.5. Ricin detection using stabilized reagent

Three sdAbs with improved T_m (D12fneg, H1W, and C10neg) were incorporated as sandwich pairs into MagPlex bead-based assays for the detection of ricin (Fig. 6). Each of the sdAbs was used as both a bead-immobilized capture and a biotinylated reporter. To increase the signal intensities, the assays were amplified by addition of Bt-goat anti-streptavdin following the first addition of SAPE, followed by a second incubation of SAPE. These steps were found to increase the signal level by a factor of ~5, and unlike

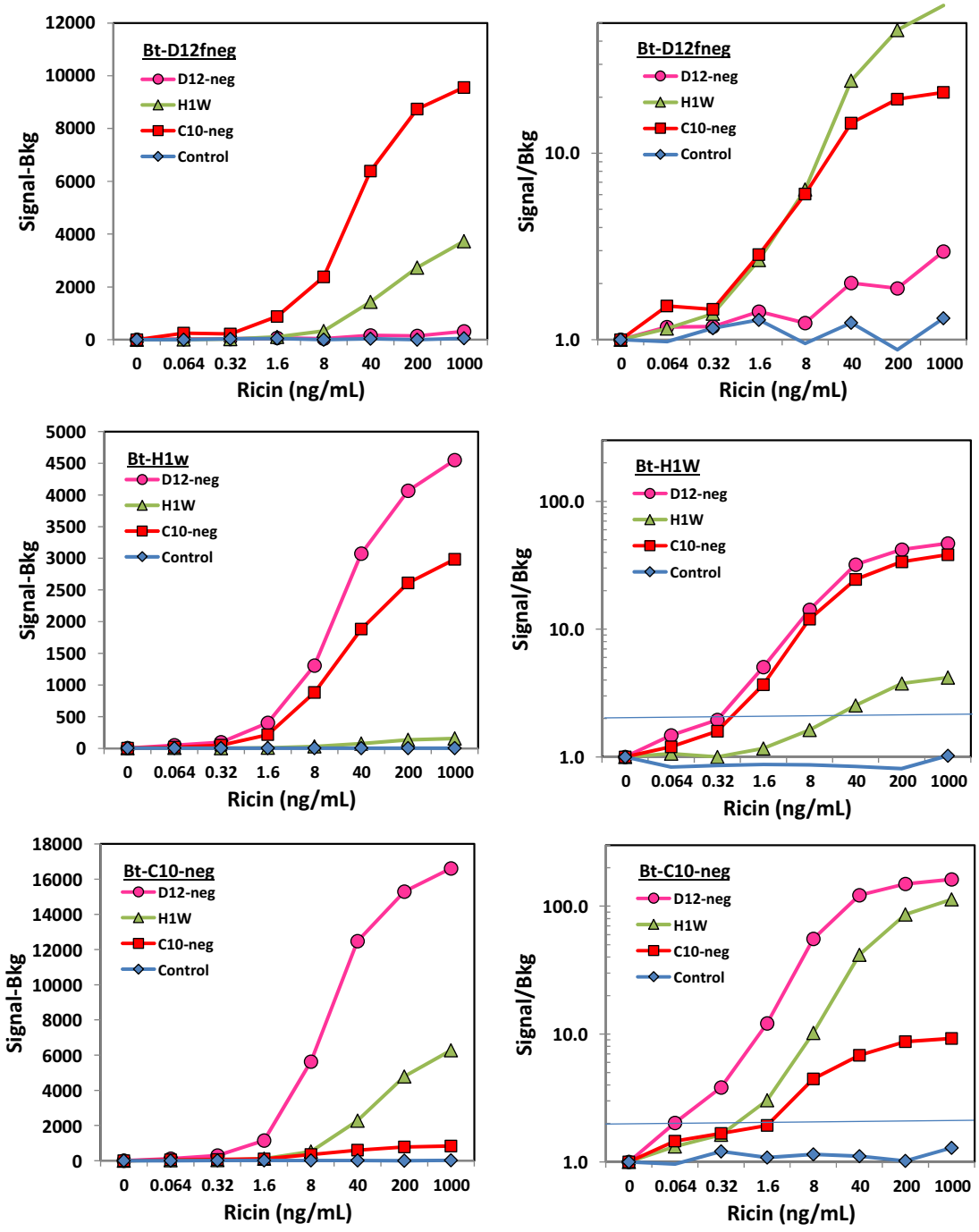

Fig. 6. Amplified bead based detection of ricin using thermal stabilized sdAbs. Shown on the left side are plots of signal minus background, with the same data shown as log plots of signal/background on the right to better visualize the response to low levels of ricin. See Section 2.10 for assay details.

earlier work where no improvement in signal to background was achieved [36], a 5-fold increase in sensitivity versus unamplified assays was obtained (Supplemental Fig. 2). The D12fneg/Bt-C10neg sdAb pair was demonstrated to be as effective as our previously reported sdAbs for toxin detection. The amplification step for these negatively modified sdAbs was likely necessary to overcome the reduced biotinylation level for the detection sdAb, as the biotinylation reagent is amine directed.

It is important to ensure that biotinylating the sdAbs to produce the reporter reagents does not negatively impact their T_m values. Using biotinylated preparations of D12fneg and C10neg, we performed CD analysis and confirmed that the T_m of the biotinylated and unbiotinylated sdAbs were identical (not shown).

4. Conclusions

We have demonstrated how a combination of thorough evaluation of clonal variants available followed by consensus sequence mutagenesis, negative mutations to improve solubility, and Cys mutations to promote an additional disulfide can lead to sdAbs with improved aggregation resistance and elevated T_ms. Decreasing aggregation and improving stability are properties that may also be beneficial for sdAbs developed as therapeutics [41]. We had previously shown that in addition to its potential use as a detection reagent, the sdAb C8 was found to inhibit ricin's biological activity [26]. As D12 and C8 are in the same sequence family, the improved anti-ricin sdAbs may also prove to have value as therapeutic reagents.

This work demonstrated a road-map for improving the utility of three sdAbs each of which binds a distinct epitope on ricin. In each case we achieved a substantial increase in T_m over C8, H1, and D1, the sdAbs that had previously been selected for the development of ricin immunoassays.

Acknowledgements

The work presented in this paper was funded by the Defense Threat Reduction Agency and NRL base 6.1 and 6.2 funds.

Appendix A. Supplementary data

Supplementary data associated with this article can be found, in the online version, at http://dx.doi.org/10.1016/j.btre.2015.01.001.

References

[1] M.A. Ghahroudi, A. Desmyter, L. Wyns, R. Hamers, S. Muyldermans, Selection and identification of single domain antibody fragments from camel heavy-chain antibodies, FEBS Lett. 414 (1997) 521–526.
[2] J. Wesolowski, V. Alzogaray, J. Reyelt, M. Unger, K. Juarez, M. Urrutia, A. Cauerhff, W. Danquah, B. Rissiek, F. Scheuplein, N. Schwarz, S. Adriouch, O. Boyer, M. Seman, A. Licea, D.V. Serreze, F.A. Goldbaum, F. Haag, F. Koch-Nolte, Single domain antibodies: promising experimental and therapeutic tools in infection and immunity, Med. Microbiol. Immunol. 198 (2009) 157–174.
[3] L. Eyer, K. Hruska, Single-domain antibody fragments derived from heavy-chain antibodies: a review, Vet. Med. 57 (2012) 439–513.
[4] A. de Marco, Biotechnological applications of recombinant single-domain antibody fragments, Microb. Cell Fact. 10 (2011) 44.
[5] S. Ewert, C. Cambillau, K. Conrath, A. Pluckthun, Biophysical properties of camelid V-HH domains compared to those of human V(H) 3 domains, Biochemistry 41 (2002) 3628–3636.
[6] E.R. Goldman, G.P. Anderson, J.L. Liu, J.B. Delehanty, L.J. Sherwood, L.E. Osborn, L.B. Cummins, A. Hayhurst, Facile generation of heat-stable antiviral and antitoxin single domain antibodies from a semisynthetic llama library, Anal. Chem. 78 (2006) 8245–8255.
[7] Y. Akazawa-Ogawa, M. Takashima, Y.H. Lee, T. Ikegami, Y. Goto, K. Uegaki, Y. Hagihara, Heat-induced irreversible denaturation of the camelid single domain VHH antibody is governed by chemical modifications, J. Biol. Chem. 289 (2014) 15666–15679.
[8] A.W.P. Vermeer, W. Norde, The thermal stability of immunoglobulin: unfolding and aggregation of a multi-domain protein, Biophys. J. 78 (2000) 394–404.
[9] E.R. Goldman, P.A. Brozozog-Lee, D. Zabetakis, K.B. Turner, S.A. Walper, J.L. Liu, G.P. Anderson, Negative tail fusions can improve ruggedness of single domain antibodies, Protein Express. Purif. 95 (2014) 226–232.
[10] S.A. Walper, S.R. Battle, P.A.B. Lee, D. Zabetakis, K.B. Turner, P.E. Buckley, A.M. Calm, H.S. Welsh, C.R. Warner, M.A. Zacharko, E.R. Goldman, G.P. Anderson, Thermostable single domain antibody-maltose binding protein fusion for *Bacillus anthracis* spore protein BclA detection, Anal. Biochem. 447 (2014) 64–73.
[11] J.M. Perchiacca, M. Bhattacharya, P.M. Tessier, Mutational analysis of domain antibodies reveals aggregation hotspots within and near the complementarity determining regions, Protein Struct. Funct. Bioinf. 79 (2011) 2637–2647.
[12] J.M. Perchiacca, A.R.A. Ladiwala, M. Bhattacharya, P.M. Tessier, Aggregation-resistant domain antibodies engineered with charged mutations near the edges of the complementarity-determining regions, Protein Eng. Des. Sel. 25 (2012) 591–601.
[13] K. Dudgeon, R. Rouet, I. Kokmeijer, P. Schofield, J. Stolp, D. Langley, D. Stock, D. Christ, General strategy for the generation of human antibody variable domains with increased aggregation resistance, Proc. Natl. Acad. Sci. U. S. A. 109 (2012) 10879–10884.
[14] A.E. Miklos, C. Kluwe, B.S. Der, S.P. Pai, A. Sircar, R.A. Hughes, M. Berrondo, J.Q. Xu, V. Codrea, P.E. Buckley, A.M. Calm, H.S. Welsh, C.R. Warner, M.A. Zacharko, J.P. Carney, J.J. Gray, G. Georgiou, B. Kuhlman, A.D. Ellington, Structure-based design of supercharged, highly thermoresistant antibodies, Chem. Biol. 19 (2012) 449–455.
[15] B.S. Der, C. Kluwe, A.E. Miklos, R. Jacak, S. Lyskov, J.J. Gray, G. Georgiou, A.D. Ellington, B. Kuhlman, Alternative computational protocols for supercharging protein surfaces for reversible unfolding and retention of stability, PLoS One 8 (5) (2013) e64363.
[16] J.M. Perchiacca, C.C. Lee, P.M. Tessier, Optimal charged mutations in the complementarity-determining regions that prevent domain antibody aggregation are dependent on the antibody scaffold, Protein Eng. Des. Sel. 27 (2014) 29–39.
[17] K.B. Turner, D. Zabetakis, E.R. Goldman, G.P. Anderson, Enhanced stabilization of a stable single domain antibody for SEB toxin by random mutagenesis and stringent selection, Protein Eng. Des. Sel. 27 (2014) 89–95.
[18] D. Zabetakis, G.P. Anderson, N. Bayya, E.R. Goldman, Contributions of the complementarity determining regions to the thermal stability of a single-domain antibody, PLoS One 8 (10) (2013) e76834.
[19] D. Saerens, M. Pellis, R. Loris, E. Pardon, M. Dumoulin, A. Matagne, L. Wyns, S. Muyldermans, K. Conrath, Identification of a universal VHH framework to graft non-canonical antigen-binding loops of camel single-domain antibodies, J. Mol. Biol. 352 (2005) 597–607.
[20] S. Ewert, A. Honegger, A. Pluckthun, Stability improvement of antibodies for extracellular and intracellular applications: CDR grafting to stable frameworks and structure-based framework engineering, Methods 34 (2004) 184–199.
[21] A.D. McConnell, V. Spasojevich, J.L. Macomber, I.P. Krapf, A. Chen, J.C. Sheffer, A. Berkebile, R.A. Horlick, S. Neben, D.J. King, P.M. Bowers, An integrated approach to extreme thermostabilization and affinity maturation of an antibody, Protein Eng. Des. Sel. 26 (2013) 151–163.
[22] Y. Hagihara, S. Mine, K. Uegaki, Stabilization of an immunoglobulin fold domain by an engineered disulfide bond at the buried hydrophobic region, J. Biol. Chem. 282 (2007) 36489–36495.
[23] D. Saerens, K. Conrath, J. Govaert, S. Muyldermans, Disulfide bond introduction for general stabilization of immunoglobulin heavy-chain variable domains, J. Mol. Biol. 377 (2008) 478–488.
[24] G. Hussack, T. Hirama, W. Ding, R. MacKenzie, J. Tanha, Engineered single-domain antibodies with high protease resistance and thermal stability, PLoS One 6 (11) (2011) e28218.
[25] Y. Hagihara, D. Saerens, Engineering disulfide bonds within an antibody, Biochim. Biophys. Acta 1844 (2014) 2016–2023.
[26] G.P. Anderson, J.L. Liu, M.L. Hale, R.D. Bernstein, M. Moore, M.D. Swain, E.R. Goldman, Development of antiricin single domain antibodies toward detection and therapeutic reagents, Anal. Chem. 80 (2008) 9604–9611.
[27] G.P. Anderson, R.D. Bernstein, M.D. Swain, D. Zabetakis, E.R. Goldman, Binding kinetics of antiricin single domain antibodies and improved detection using a B chain specific binder, Anal. Chem. 82 (2010) 7202–7207.
[28] S. Olsnes, Ricin and ricinus agglutinin, toxic lectins from castor bean, Methods Enzymol. 50 (1978) 330–335.
[29] L.D. Rotz, A.S. Khan, S.R. Lillibridge, S.M. Ostroff, J.M. Hughes, Public health assessment of potential biological terrorism agents, Emerg. Infect. Dis. 8 (2002) 225–230.
[30] R.B. Reisler, L.A. Smith, The need for continued development of ricin countermeasures, Adv. Prev. Med. 2012 (2012) 149737.
[31] M. Cummins, C. Dogovski, R. Robert, M. Alderton, D. Chong, D. Proll, L. Pontes-Braz, A. Raicevic, M. Hattarki, S. Nuttall, O. Dolezal, Kinetic characterization of a panel of high-affinity monoclonal antibodies targeting ricin and recombinant re-formatting for biosensor applications, Antibodies 3 (2014) 215–231.
[32] F. Corpet, Multiple sequence alignment with hierarchical-clustering, Nucleic Acids Res. 16 (1988) 10881–10890.
[33] K.B. Turner, D. Zabetakis, P. Legler, E.R. Goldman, G.P. Anderson, Isolation and epitope mapping of staphylococcal enterotoxin B single-domain antibodies, Sensors (Basel) 14 (2014) 10846–10863.
[34] J.L. Liu, D. Zabetakis, E.R. Goldman, G.P. Anderson, Selection and evaluation of single domain antibodies toward MS2 phage and coat protein, Mol. Immunol. 53 (2013) 118–125.

[35] S.A. Walper, P.A.B. Lee, G.P. Anderson, E.R. Goldman, Selection and characterization of single domain antibodies specific for *Bacillus anthracis* spore proteins, Antibodies 2 (2013) 152–167.
[36] G. Anderson, C. Taitt, Suspension microarray immunoassay signal amplification using multilayer formation, Sensor Lett. 6 (2008) 213–218.
[37] S.A. Walper, G.P. Anderson, P.A.B. Lee, R.H. Glaven, J.L. Liu, R.D. Bernstein, D. Zabetakis, L. Johnson, J.M. Czarnecki, E.R. Goldman, Rugged single domain antibody detection elements for *Bacillus anthracis* spores and vegetative cells, PLoS One 7 (3) (2012) e32801.
[38] N. Wang, W.E. Smith, B.R. Miller, D. Aivazian, A.A. Lugovskoy, M.E. Reff, S.A. Glaser, L.J. Croner, S.J. Demarest, Conserved amino acid networks involved in antibody variable domain interactions, Protein Struct. Funct. Bioinf. 76 (2009) 99–114.
[39] S.A. Walper, J.L. Liu, D. Zabetakis, G.P. Anderson, E.R. Goldman, Development and evaluation of single domain antibodies for vaccinia and the L1 antigen, PLoS One 9 (9) (2014) e106263, doi:http://dx.doi.org/10.1371/journal.pone.0106263.
[40] D. Zabetakis, M.A. Olson, G.P. Anderson, P.M. Legler, E.R. Goldman, Evaluation of disulfide bond position to enhance the thermal stability of a highly stable single domain antibody, PLoS One 9 (12) (2014) e115405.
[41] J.D. Unciti-Broceta, T. Del Castillo, M. Soriano, S. Magez, J.A. Garcia-Salcedo, Novel therapy based on camelid nanobodies, Ther. Deliv. 4 (2013) 1321–1336.